21st Australasian Fluid Mechanics Conference
Adelaide, Australia
10-13 December 2018

Sound Generation by Planar, CH4/Air Flame Annihilation with Several Chemical Mechanisms

D. Brouzet[1], X. Dou[1], M. Talei[1], R. L. Gordon[1] and M. J. Brear[1]

[1]Department of Mechanical Engineering,
University of Melbourne, Parkville, VIC, 3010, Australia

Abstract

This paper investigates the importance of chemical modelling on the sound generation by planar, premixed laminar flame annihilation. A stoichiometric, methane/air flame at atmospheric pressure and unburnt gas temperature of 300K is considered with four different chemical mechanisms of increasing complexity [6, 11, 4, 15].

The laminar flame speeds obtained from these different mechanisms are first found to be very similar and consistent with the literature. However, differences in their heat release rate profiles lead to differing pressure fluctuations in the far field. Specifically, when more complex mechanisms are used, the later stages of the annihilation process are characterized by a slower decrease of the heat release rate which, in turn, affects the radiated pressure fluctuations. Analysis of the contribution of the reaction rates of different species then shows that it is essential to model CO to CO2 oxidation accurately in the post-flame region in order to accurately model the acoustics. Nonetheless, the overall pressure difference between the burnt and unburnt gases is found to be independent of the mechanism since, as the theory of Talei et al. [17] showed, this only depends on the flame speed and the flame temperature.

Introduction

Lean premixed combustion is a promising method to decrease nitrogen oxide emissions in modern gas turbines. However, the combustors operating under lean conditions are susceptible to the so called thermo-acoustic instabilities [13]. This resonance phenomenon involves a strong coupling between the flame dynamics and the acoustic waves and results in large pressure fluctuations, leading to the combustor failure in extreme cases [12, 16]. As a result, achieving an improved understanding of premixed flame acoustics is of great importance for environmental and safety reasons.

The fluctuations of the heat release rate $\dot{Q}$ have been shown to be the acoustics leading cause in reacting flows [5, 9]. One mechanism that can lead to large fluctuations of $\dot{Q}$ is flame annihilation. When two flame surfaces approach each other, the unburned gas trapped between them is rapidly consumed, resulting in large fluctuations of the heat release rate. Their contribution to the acoustics has been shown in experimental studies of forced laminar premixed flame [3, 14]. Candel et al. [3] have even argued that they could be a major source of noise in turbulent combustors. Schuller et al. [14] have also showed that the acoustics induced by annihilation events could lead to self sustained oscillations of the flame front, if the pressure fluctuations were in phase with the velocity fluctuations at the burner's inlet. This result therefore shows the potential implication of annihilation events in flame instabilities.

Following these investigations, Talei et al. [17, 18] have highlighted the importance of flame annihilation in the sound generation process for one-dimensional (1-D) premixed flames. They developed a theoretical framework for calculating the sound produced by planar, axisymmetric and spherically symmetric annihilation events. In subsequent direct numerical simulation (DNS) studies, annihilation events were observed to be a significant source of noise in two-dimensional (2-D) forced laminar premixed flames. More recently, Haghiri et al. [8] analysed the acoustics from three-dimensional (3-D) turbulent premixed flames. Their simple acoustic model based on flame annihilations highlighted their contribution to the overall sound generation. However, all those studies used simple chemistry schemes to perform their DNS.

Jimenez et al. [10] have done a comparison of the sound generated by 1-D H2/air premixed flame annihilation, using simple and detailed chemistry. They found that the simple chemistry was predicting accurately the pressure fluctuation amplitude for Lewis number smaller or equal to unity. On the other hand, Ghani & Poinsot [7] found that simple kinetics for CH4/air stoichiometric flames resulted in a significant over-estimation of the pressure amplitude, in a 1-D head on quenching configuration. This difference was explained by a too fast extinction of the heat release rate after quenching, as the simple mechanism did not take into account the kinetics of minor and intermediate species.

Overall, few studies have analysed the effect of chemistry on the sound generation process in premixed flames. The goal of this paper is to examine and explain the acoustic differences due to different chemistry mechanisms, for a 1-D CH4/air flame annihilation. For this purpose, 4 different schemes, with various complexity, are used to model the chemistry.

DNS dataset

The DNS were performed using the code for reacting flows NTMIX-CHEMKIN. The complete set of equations and the species molecular transport model used can be found in Baum et al. [1]. NTMIX-CHEMKIN uses a 8^{th} order central differencing scheme with a 3^{rd} order Runge-Kutta algorithm and a 10^{th} order filtering scheme. The simulations represent a 1-D laminar CH4/air premixed flame annihilation with an unburned gas temperature $T_u = 300K$ and an equivalence ratio $\phi = 1$ at atmospheric pressure. A stretched grid with a total of 2500 points was used on the $600\delta_{th}$-long domain, where δ_{th} represents the thermal flame thickness. The stretching ratio was kept under 0.5% and at least 40 points per δ_{th} was used in the reaction zone. The 1-D NSCBC adapted to reacting flows [2] is applied at the outlet while a symmetry condition is used at the lower boundary (fig. 1), so that only half the domain had to be computed.

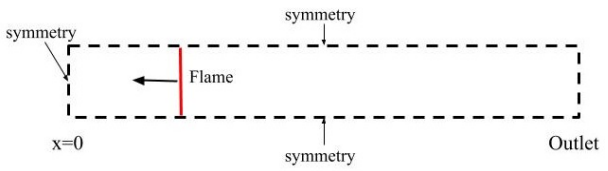

Figure 1: Sketch of DNS configuration.

If not specified otherwise, the results presented are non-

dimensionalized by the reference values of speed $c_{ref} = 353\ m/s$, density $\rho_{ref} = 1.12\ kg/m^3$ and temperature $T_{ref} = 116\ K$. The reference length is set up to $10\delta_{th}$, based on the GRI3.0 flame, so that $L_{ref} = 4.81\ mm$. The annihilation time, instant when the peak of heat release rate reaches the symmetry line, is taken as reference $t = 0$.

Four chemistry mechanisms were used, namely the 2-steps BFER (2S-BFER) [6], 4-steps Jones & Lindstedt (J&L) [11], 39-reactions Coffee [4] and 325-reactions GRI 3.0 [15] schemes (see table 1). The reduced 2S-BFER mechanism has been validated for a range of unburnt gas temperature (300K to 700K), pressure (1 atm to 15 atm) and equivalence ratio (0.6 to 1.4) by comparing the laminar flame speed and adiabatic temperature to GRI3.0 results. The J&L scheme is a global reaction scheme for hydrocarbons, featuring a two-reaction zone flame model. It has been validated against experimental data for methane/air premixed flames by analysing the laminar flame speed and the main species profiles, for $\phi = 0.85$ to $\phi = 1.25$. The Coffee scheme as been also validated with experimental data of premixed methane/air flames at $T_u = 300K$ and atmospheric pressure. Species and temperature profiles, as well as laminar flame speed, were compared for equivalence ratios from 0.85 to 1.25. The GRI3.0 mechanism is the most complex one and taken as reference in this study.

Scheme	Species #	Reactions #
2S-BFER	6	2
J&L	7	4
Coffee	14	38
GRI 3.0	53	325

Table 1: Chemistry schemes characteristics.

Results

Table 2 shows the laminar flame speed S_L obtained with the different mechanisms. Overall, there are in accordance with the values from the literature. Figure 2 shows the heat release rate profile for the freely propagating flame. Coffee (dot-dashed line) and GRI3.0 (solid line) are extremely similar, with the former having a slightly larger peak amplitude. The heat release rate obtained with the 2S-BFER mechanim (dotted line) decreases quickly to zero in the post-flame region, while the more complex mechanisms feature a non-negligible $\dot{Q}$. This can be explained by the lack of intermediate or minor species in the 2-steps mechanism. Note the J&L mechanism (dashed line) manages to capture partially the slow decrease in the post-flame region, as it features a secondary reaction zone, where oxidation to CO2 occurs.

Scheme	S_L in this study	S_L from literature
2S-BFER	40.5	40.6 [6]
J&L	41.8	40.9 [11]
Coffee	39.9	39.7 [4]
GRI 3.0	37.4	37.9 [15]

Table 2: Laminar flame speed S_L in cm/s for the mechanisms considered in this paper.

The flame speed U_f, normalized by S_L, is shown in fig. 3 for the instants before the annihilation time. The flame's position was estimated based of the heat release rate peak and its speed computed through a 1^{st} order numerical central difference scheme. Despite the differences between the mechanisms, the flame's acceleration prior to annihilation is well predicted by all of them.

The pressure fluctuations induced by the annihilation event are

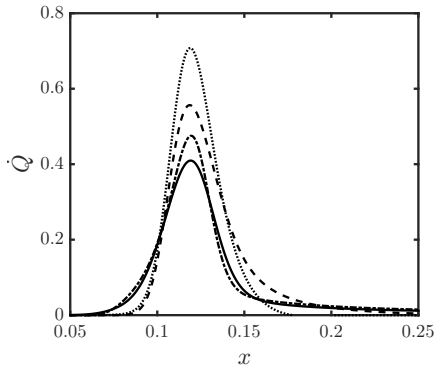

Figure 2: Heat release rate of the freely propagating flame for 2S-BFER (dotted line), J&L (dashed line), Coffee (dot-dashed line) and GRI3.0 (solid line).

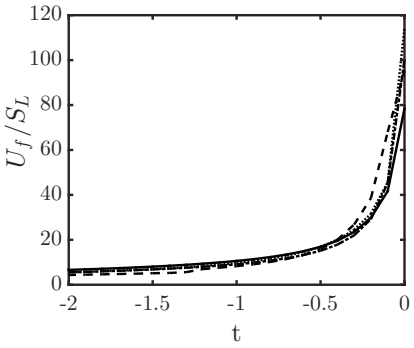

Figure 3: Flame displacement speed before annihilation for 2S-BFER (dotted line), J&L (dashed line), Coffee (dot-dashed line) and GRI3.0 (solid line).

now analysed. In the following, the pressure before annihilation p_∞ is taken as reference. First of all, the total pressure difference Δp induced at the symmetry line is shown in table 3, from the numerical results and the theory from Talei et al. [17]:

$$\Delta p = -\rho_u c_b (1 - T_u/T_b) S_L\ , \qquad (1)$$

where the subscript $_b$ refers to the values in the burnt gases. The numerical results are in accordance with the theoretical values. Furthermore, all schemes have similar values, showing that even simplified chemistries can predict accurately the far-field sound pressure level in this configuration.

The spatial shape of the pressure waves in the far-field are now discussed (fig 4). All mechanisms, except J&L, feature first a small positive pressure peak. Then, the pressure abruptly decreases. While the 2S-BFER pressure (dotted line) remains steady, the other mechanisms feature a slower decrease. We will show now that this result is linked to the heat release rate post-flame behaviour, discussed in fig. 2.

Scheme	Δp from eq. 1	Numerical Δp	Difference
2S-BFER	2.78E-3	2.45E-3	11.8 %
J&L	2.77E-3	2.44E-3	11.7%
Coffee	2.64E-3	2.55E-3	3.5%
GRI 3.0	2.49E-3	2.22E-3	10.8%

Table 3: Pressure difference Δp obtained with several schemes.

It can be shown [17] that in a 1-D planar case, the pressure

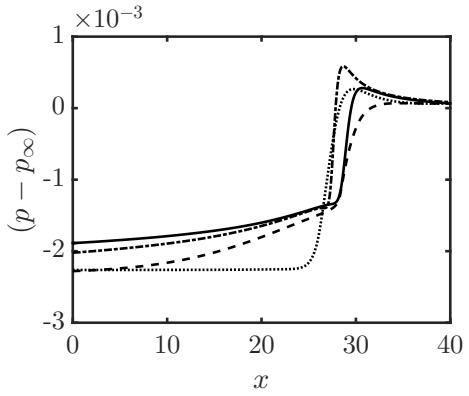

Figure 4: Pressure fluctuations in the far-field after annihilation for 2S-BFER (dotted line), J&L (dashed line), Coffee (dot-dashed line) and GRI3.0 (solid line).

fluctuation at a point x in the far-field and time t is given by

$$p'(x,t) = \frac{c_u}{2}\left(1-\frac{T_u}{T_b}\right)\int_V \dot{Q}\,(V_0, t-|\,x\,|/c_b)\,dV_0\ , \qquad (2)$$

where V_0 represents the flame's region, i.e. where $\dot{Q}$ is non-zero. Equation 1 shows that, in a planar configuration, the acoustics are proportional to the integral of heat release rate. Figure 5 shows the temporal evolution of the heat release rate for the four mechanisms. The fast $\dot{Q}$ decrease after $t = 0$ is obvious for the 2S-BFER mechanism (top left). On the other hand, the peak in the post-flame region, representing the secondary reaction zone, can be noticed in the J&L case (top right). Overall, the slower and minor reactions present in the more complex mechanisms (J&L, Coffee and GRI3.0) explain the slower decay of heat release rate after $t = 0$, and therefore the pressure behaviour from fig. 4.

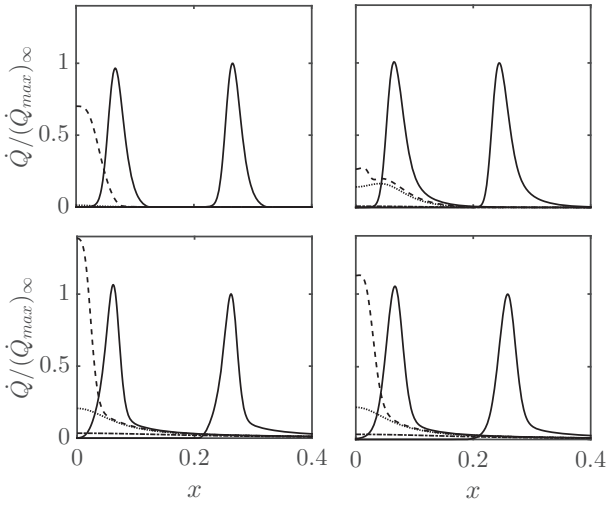

Figure 5: Heat release rate profiles for 2S-BFER (top left), J&L (top right), Coffee (bottom left) and GRI3.0 (bottom right). The lines represent different time instants: freely propagating flame (solid line far right), $t = -7$ (left solid line), $t = 0$ (dashed line), $t = 0.5$ (dotted line) and $t = 5$ (dot-dashed line).

We are now comparing in more details the 2S-BFER and J&L mechanisms in order to establish which reactions are necessary to predict more realistically the heat release rate decay. 2S-BFER comprises the following reactions:

$$CH_4 + 1.5O_2 \Rightarrow \quad CO + 2H_2O \qquad (3)$$
$$CO + 0.5O_2 \Leftrightarrow \quad CO_2 \qquad (4)$$

while J&L has the 4 following steps:

$$CH_4 + 0.5O_2 \Rightarrow \quad CO + 2H_2 \qquad (5)$$
$$CH_4 + H_2O \Rightarrow \quad CO + 3H_2 \qquad (6)$$
$$H_2 + 0.5O_2 \Leftrightarrow \quad H_2O \qquad (7)$$
$$CO + H_2O \Leftrightarrow \quad CO_2 + H_2 \qquad (8)$$

Figure 6 represents the contribution from the main species to the overall heat release rate, at several instants. By analysing the 2S-BFER results (left column), it can be seen that there is only one reaction rate peak, that coincide with the overall heat release rate. This results in a complete consumption of reactants after the flame reaches the symmetry point. On the other hand, the J&L mechanism (right column) features a first peak of reactants for CH4 (orange line) and CO (blue line) in the pre-heat region, caused by reactions 6 and 7. The overall heat release rate peak is associated with the H2O production (green line) in reaction 8 and production of CO2 (purple line) by reaction 8 explains the heat release rate decay in the secondary reaction zone.

The results at $t = 0$ and $t = 0.5$ show that this latest reaction is responsible for the heat release rate behaviour after annihilation time. Even if the CO to CO2 oxidation was taken into account in the 2S-BFER scheme, the overall mechanism did not capture the secondary reaction zone, contrary to J&L, Coffee and GRI3.0. These results suggest that a realistic representation of CO oxidation is necessary to predict accurately the heat release rate and pressure behaviour when considering a planar premixed flame.

Conclusions

This paper investigated the importance of chemical modelling on the sound generation by planar, premixed laminar flame annihilation. A stoichiometric, methane/air flame at atmospheric pressure and unburnt gas temperature of 300K was considered with four different chemical mechanisms of increasing complexity [6, 11, 4, 15].

The flame speeds obtained from these different mechanisms were first found to be very similar and consistent with the literature, showing that the flame kinematics were well predicted by all mechanisms. However, differences in their heat release rate profiles led to differing pressure fluctuations in the far field. Specifically, when more complex mechanisms were used, the later stages of the annihilation process were characterized by a slower decrease of the heat release rate which, in turn, affected the radiated pressure fluctuations. Analysis of the contribution of the reaction rates of different species then showed that it is essential to model CO to CO2 oxidation accurately in the post-flame region in order to accurately model the acoustics. Nonetheless, the overall pressure difference between the burnt and unburnt gases was found to be independent of the mechanism since, as the theory of Talei et al. [17] showed, this only depends on the flame speed and the flame temperature.

As the relation between the heat release rate and the far-field acoustics changes in axisymmetric and spherically symmetric flames, a similar study in higher dimensions could give more insight into the limitations of some mechanisms in more realistic configurations. For instance, in a 3-D domain, the pressure fluctuations are proportional to the time derivative of heat release rate $\partial\dot{Q}/\partial t$. It is still unclear if slow reactions occurring in

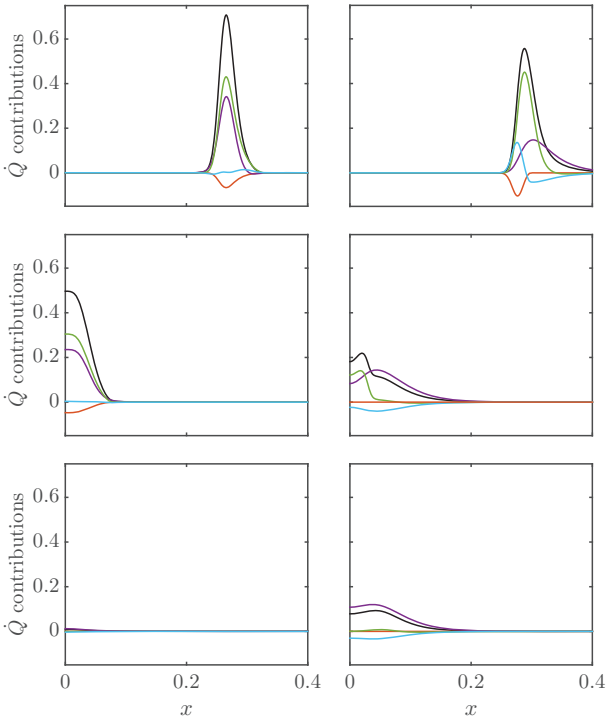

Figure 6: Heat release rate contributions for 2S-BFER (left column) and J&L (right column), for the freely propagating flame (top row), at $t = 0$ (middle row) and $t = 0.5$ (bottom row). The coloured lines represent the contributions from CH4 (orange), CO2 (purple), H2O (green) and CO (blue). Overall $\dot{Q}$ is shown by the solid black line.

the post-flame region will matter to predict accurately the generated sound. Future work will investigate the significance of these findings for 3-D turbulent premixed flames.

Acknowledgements

This work was supported by the Australian Research Council. The research benefited from computational resources provided through the National Computational Merit Allocation Scheme, supported by the Australian Government. The computational facilities supporting this project included the Australian NCI National Facility and the Pawsey Supercomputing Center.

References

[1] Baum, M., Poinsot, T., Haworth, D. and Daraviha, N., Direct numerical simulation of H2/O2/N2 flames with complex chemistry in two-dimensional turbulent flows, *J. Fluid Mech.*, **281**, 1994, 1–32.

[2] Baum, M., Poinsot, T. and Thevenin, D., Accurate boundary conditions for multicomponent reactive flows, *J. Comput. Phys.*, **116**, 1995, 247–261.

[3] Candel, S., Durox, D. and Schuller, T., Flame interactions as a source of noise and combustion instabilities, *10th AIAA/CEAS Aeroacoustics Conf.*, 2928.

[4] Coffee, T. P., Kinetic mechanisms for premixed , laminar, steady state methane/air flames, *Combust. Flame*, **55**, 1984, 161–170.

[5] Dowling, A. P., Thermoacoustic sources and instabilities, in *Modern Methods in Analytical Acoustics*, Springer-Verlag, 1992, volume 92, 378–405.

[6] Franzelli, B., Riber, E., Gicquel, L. and Poinsot, T., Large eddy simulation of combustion instabilities in a lean partially premixed swirled flame, *Combust. Flame*, **159**, 2012, 621–637.

[7] Ghani, A. and Poinsot, T., Flame quenching at walls: A source of sound generation, *Flow, Turbul. Combust.*, **99**, 2017, 173–184.

[8] Haghiri, A., Talei, M., Brear, M. J. and Hawkes, E. R., Sound generation by turbulent premixed flames, *J. Fluid Mech.*, **843**, 2018, 29–52.

[9] Ihme, M., Combustion and engine-core noise, *Annu. Rev. Fluid Mech.*, **49**, 2017, 227–310.

[10] Jimenez, C., Haghiri, A., Brear, M. J., Talei, M. and Hawkes, E. R., Sound generation by premixed flame annihilation with full and simple chemistry, *Proc. Combust. Inst.*, **35**, 2015, 3317–3325.

[11] Jones, W. P. and Lindstedt, R. P., Global reaction schemes for hydrocarbon combustion, *Combust. Flame*, **73**, 1988, 233–249.

[12] Nicoud, F. and Poinsot, T., Thermoacoustic instabilities: Should the Rayleigh criterion be extended to include entropy changes?, *Combust. Flame*, **142**, 2005, 153–159.

[13] Poinsot, T. and Veynante, D., *Theoretical and Numerical Combustion*, RT Edwards, Inc., 2005, third edition.

[14] Schuller, T., Durox, D. and Candel, S., Self-induced combustion oscillations of laminar premixed flames stabilized on annular burners, *Combust. Flame*, **135**, 2003, 525–537.

[15] Smith, G., Golden, D., Frenklach, M., Moriarty, N., Eiteneer, B., Goldenberg, M., Bowman, C., Hanson, R., Song, S., Gardiner Jr., W., Lissianski, V. and Qin, Z., http://www.me.berkeley.edu/gri_mech/.

[16] Swaminathan, N., Xu, G., Dowling, A. P. and Balachandran, R., Heat release rate correlation and combustion noise in premixed flames, *J. Fluid Mech.*, **681**, 2011, 80–115.

[17] Talei, M., Brear, M. J. and Hawkes, E. R., Sound generation by laminar premixed flame annihilation, *J. Fluid Mech.*, **679**, 2011, 194–218.

[18] Talei, M., Brear, M. J. and Hawkes, E. R., A parametric study of sound generation by premixed laminar flame annihilation, *Combust. Flame*, **159**, 2012, 757–769.

[19] Talei, M., Hawkes, E. R. and Brear, M. J., A direct numerical simulation study of frequency and Lewis number effects on sound generation by two-dimensional forced laminar premixed flames, *Proc. Combust. Inst.*, **34**, 2013, 1093–1100.